This is the Pre-Published Version.

Y. Qin, Y. Chen, S. Lin, X. Huang (2022) *Limiting Oxygen Concentration and Supply Rate of Smoldering Propagation*, **Combustion and Flame**, 245, 112380. https://doi.org/10.1016/j.combustflame.2022.112380

Limiting Oxygen Concentration and Supply Rate of Smoldering Propagation

Yunzhu Qin [1], Yuying Chen [1], Shaorun Lin [1,2,*], Xinyan Huang [1,*]

[1] *Research Centre for Fire Safety Engineering, Department of Building Environment and Energy Engineering, The Hong Kong Polytechnic University, Hong Kong*

[2] *The Hong Kong Polytechnic University Shenzhen Research Institute, Shenzhen, China*

**Corresponding authors: xy.huang@polyu.edu.hk (X.H) and shaorun.lin@outlook.com (S.L)*

Abstract

Smoldering combustion of porous fuel is a slow, low-temperature, and flameless process that is sustained by heterogenous oxidations. The influence of oxygen supply on smoldering propagation is of vital significance but still not fully understood. This work explores the smoldering propagation on peat soil under an internal oxidizer flow with velocity up to 14.7 mm/s and oxygen concentration of 2 - 21%. After ignition in the middle of the fuel bed, by decreasing the internal airflow velocity, the smoldering propagation changes from bidirectional (forward + opposed) to unidirectional (opposed). Further reducing the airflow velocity to 0.3 mm/s, no propagation occurs with a minimum smoldering temperature of about 300 ºC. As the internal flow velocity increases, the limiting oxygen concentration for smoldering decreases and approach to a minimum value that is below 2%. The minimum oxygen supply rate for smoldering approaches a constant of 0.08 ± 0.01 g/m^2·s, when the oxygen concentration is larger than 10%. Further reducing the oxygen concentration below 10%, the required minimum rate of oxygen supply increases significantly, because of the enhanced convection cooling by a larger internal flow velocity. This work quantifies the minimum oxygen supply for the smoldering combustion and advances the fundamental understanding of the persistence of smoldering propagation in underground peat layers.

Keywords: smoldering combustion; peat fire; propagation pattern; flow velocity; oxygen limit

1. Introduction

Smoldering combustion is slow, low-temperature, and flameless that is driven by exothermic heterogeneous oxidations when oxygen molecules directly attack the hot fuel surface [1–3]. Smoldering of porous fuels can be easily initiated by a weaker heat source or even self-ignition, creating a shortcut to flaming fires through the smoldering-to-flaming transition [4]. Once ignited, smoldering can sustain in extreme conditions such as poor oxygen supply and large fuel moisture, so it is the dominant burning phenomenon in residential, industrial, and natural fires [5,6]. For example, underground peat fires can survive in deep soil layers with limited oxygen supply, resulting in long-lasting combustion phenomena on Earth [7]. On the other hand, persistent smoldering combustion has also been applied for the removal of organic wastes with a high moisture content [8–10], showing an excellent prospect for industrial application. Therefore, a better understanding of smoldering combustion is vital to mitigate the smoldering fire hazards and promote smoldering-based technologies.

Two key mechanisms control the propagation and extinction of smoldering combustion: oxygen supply and heat loss [1–3]. Among them, the influence of heat loss on smoldering propagation and extinction has been investigated systematically, and many insights are revealed, including the quenching by cold wall [11,12], moisture [13–16], and wind [17]. On the other hand, the effect of oxygen level on smoldering has been explored since the 1970s [18], but the current understanding of the oxygen supply thresholds for sustaining smoldering propagation is still limited. Schmidt et al. [19] found that in the self-ignition test, the smoldering fire could spread to the free surface at an oxygen concentration as low as 6%. Malow et al. [20] showed that lowering ambient oxygen to 5% still could not extinguish the smoldering fire on coal and wood chips.

Even for the same fuel, different values of limiting oxygen concentrations (LOC) were found in various experiments [5,21–23]. For peat, Belcher et al. [21] found that the smoldering could not be sustained below a critical oxygen concentration of 16% under natural airflow without forced oxidizer flow. However, Hadden et al. [22] found that smoldering peat fire can survive under a forced external flow at oxygen

concentrations as low as 11%. For smoldering wood, the LOC has been found to be 10% with a forced internal flow [24] and 4-6% under intense irradiation [23]. Our previous work [5] further found that the LOC of smoldering increases with the fuel moisture content. So far, the physical meaning of LOC in different smoldering experiments is still poorly understood.

Moreover, reducing the ambient pressure or gravity also lowers the oxygen supply threshold of smoldering [25–28]. The observed minimum ambient pressure for smoldering is about 10~20 kPa [27,28], similar to that of flame. Bar-Ilan et al. [25] found in microgravity spacecraft, smoldering of polyurethane foam required a smaller oxygen supply than that in normal gravity. However, the actual minimum rate of oxygen passing through the porous media is also unclear, so there is a big knowledge gap.

The oxygen supply rate into the porous fuel can be defined by the oxygen mass flux, which changes with the oxygen concentration and internal flow velocity. When a smoldering porous fuel is in contact with the ambient, the oxygen can flow into the fuel bed through pores, driven by diffusion and free convection, and such a natural oxygen supply is often sufficient for smoldering. Most past studies were performed with smoldering fuel samples open to the quiescent ambient or under an external wind, which cannot completely isolate the oxygen diffusion from the ambient. Thus, it is difficult to quantify the real minimum oxygen supply rate and LOC for smoldering combustion.

This study aims to explore the minimum internal oxygen supply rate through a porous fuel bed that is able to sustain a robust smoldering propagation. An oxidizer flow with velocity (U) up to 14.74 mm/s and oxygen concentration (X_{O_2}) of 2%-21% is fed to peat soil that is isolated from extra oxygen supply from the ambient. The total mass loss and peak temperature under different oxygen supply rates were quantified. A theoretical analysis was proposed to explain the minimum oxygen supply rate and LOC of smoldering.

2. Experimental method

2.1. Porous peat soil

The experiments choose the organic peat soil as a representative porous fuel that is prone to smoldering combustion (Fig. 1), the same as our previous studies [15,29]. Such a moss peat sample has high organic

content (~97%), uniform density, and homogenous particle size, thus ensuring better repeatability of the fire experiments. Before the tests, the peat soil was first oven-dried at 90 °C for 48 h. When the oven-dried peat was in contact with air, it quickly absorbed ambient moisture and reached a new equilibrium with ~5% moisture content [29]. However, previous studies have demonstrated that such a low moisture content has a negligible effect on the smoldering propagation [5,30]. The measured peat bulk density and porosity were 145±10 kg/m^3 and 0.90 ±0.01 [11], respectively. The shape of the peat soil is coarse, and its size is about 1 mm, leaving a large pore space between particles that allows the oxygen to pass through. Elemental analysis shows that its mass fraction of C/H/O/N/S is 45.6/6.0/48.0/0.5/0.3%, respectively. The thermogravimetric tests were conducted using PerkinElmer STA6000 under five oxygen concentrations by mixing air and N_2: 21% (air), 10%, 5%, 2% and 0% (N_2). The selected data of mass loss rate and heat flow are shown in Appendix (Fig. A1).

2.2. Experimental setup

The schematic diagram of experimental setups, which mainly consisted of a disclosed tubular smoldering reactor, an ignition system, and an oxidizer supply system, is shown in Fig. 1. The smoldering reactor was made of 2-mm thick quartz glass with a depth of 30 cm. The internal diameter of the reactor was designed to be 12 cm to minimize the quenching effect from the reactor wall [11,12]. Meanwhile, a 1-cm thick ceramic insulation layer was attached to the surface of the reactor to further reduce the environmental heat losses. To homogenize the flow from the bottom, a steel mesh was placed 3 cm above the bottom of the reactor, and a 5-cm thick layer of glass beads was poured above the steel mesh. Then, a fresh fuel sample with a constant height of 20 cm was placed on the glass beads.

An array of five K-type thermocouples (1 mm bead diameter) was inserted into the fuel with an interval of 5 cm, recording the temperature profiles with a time interval of 1 min. The coil ignitor inserted into the middle of the sample (z = 0) was used to initiate the smoldering combustion. A forced oxidizer flow was supplied from the bottom end of the reactor, and the flow rate was controlled by a flow meter with an uncertainty of 5%. A gas outlet with a diameter narrowed to 1 cm was designed on the top of the reactor to

allow the injection of emission gas and prevent the atmospheric oxygen from entering the reacting sample. Thus, the oxygen supply to the smoldering front only came from the forced oxidizer flow on the bottom.

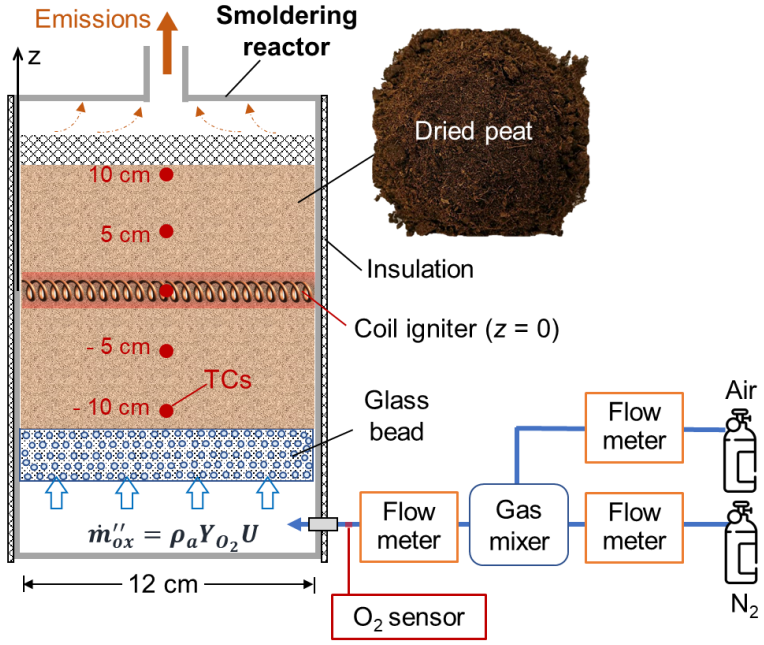

Fig. 1. Schematic diagram of experimental setup and photo of tested organic peat soil sample.

2.3. Test procedure and controlled parameters

The ignition protocol was fixed at 100 W for 15 min, which is strong enough to ignite the dry peat and start robust smoldering combustion under atmospheric conditions. Afterwards, a 1-cm layer of insulation cotton was put on the fuel surface to prevent heat loss and flying ashes. Then, the oxidizer flow with a prescribed oxygen concentration (volume fraction, X_{O_2}) and flow velocity (U) was fed from the bottom of the reactor. Herein, the oxygen supply rate is defined by the mass flux of oxygen through the cross-section of the reactor as

$$\dot{m}''_{ox} = \rho_g Y_{O_2} U \quad (1)$$

where the flow velocity (U) is an overall value for the cross-section of the reactor rather than a local velocity in pores; ρ_g is the density of oxidizer flow; $Y_{O_2}$is the oxygen mass fraction. The relationship between X_{O_2} and Y_{O_2} is $X_{O_2} = (\rho_g/\rho_{O_2})Y_{O_2}$, where the difference between X_{O_2} and Y_{O_2} is relatively small for oxygen and nitrogen mixture.

A series of tests were conducted under different oxygen supply conditions and started with normal airflow (X_{O_2} = 21%). Each test was conducted with a fresh sample under one given oxygen-supply condition. If the smoldering front can propagate in at least on direction, the flow velocity would be decreased in the follow-up tests with a fresh sample until the minimum flow velocity (U_{min}) was found. Subsequently, the value of X_{O_2} was reduced and found the relationship between X_{O_2} and U_{min}. In this work, the oxygen concentration changes from 21% to 2%, and the flow velocity changes from 0.1 mm/s to 14.7 mm/s. During the experiments, the ambient temperature was 22 ± 2 ºC, the humidity was 50±10%, and the pressure was 101 kPa. For each scenario, at least two repeating tests were conducted to ensure repeatability.

3. Results and discussion

3.1. Smoldering propagation phenomena

Fig. 2 shows the thermocouple measurements of smoldering propagations and extinction under different airflow velocities (X_{O_2} = 21%). During the ignition process by the coil heater, the temperature near the ignition zone rapidly increases above 500 ºC for all cases, so that the 15-min ignition is strong enough to initiate a robust smoldering zone.

Fig. 2(a) shows the smoldering propagation when the oxygen supply is abundant (U=4.4 mm/s). After the 15-min ignition, the gas flow was supplied from the bottom end of the reactor. The temperature first decreases but soon increases again, indicating a robust smoldering propagation [15]. Moreover, a bidirectional propagation phenomenon is shown, evident by the temperatures over 300 ºC both above (z > 0) and below (z < 0) the ignition zone. Fig. 3(a) further illustrates the ideal and simplified 1-D bidirectional propagation process under large flow velocity. As the oxygen supply is abundant, the oxygen is not fully consumed by the lower downward propagation front. Thus, the remaining oxygen can pass through to sustain the upward smoldering front, showing a bidirectional propagation mode. Similar multi-directional smoldering spread was observed in paper scraps [31] and cotton [32].

As the gas flow was provided from the bottom end, the downward (opposed) propagating smoldering front has more than sufficient oxygen supply, showing a higher smoldering temperature and propagation

rate. Comparatively, for the upward (forward) propagation, the oxygen supply is reduced, so that a lower smoldering temperature at z >0 could be observed, as shown in Fig. 2 (a). Because the oxygen supply is sufficient, the combustion of solid fuel is more complete. When all temperatures dropped to the ambient level, only a thin layer of mineral ash remained at the bottom, so the burning mass loss was maximized.

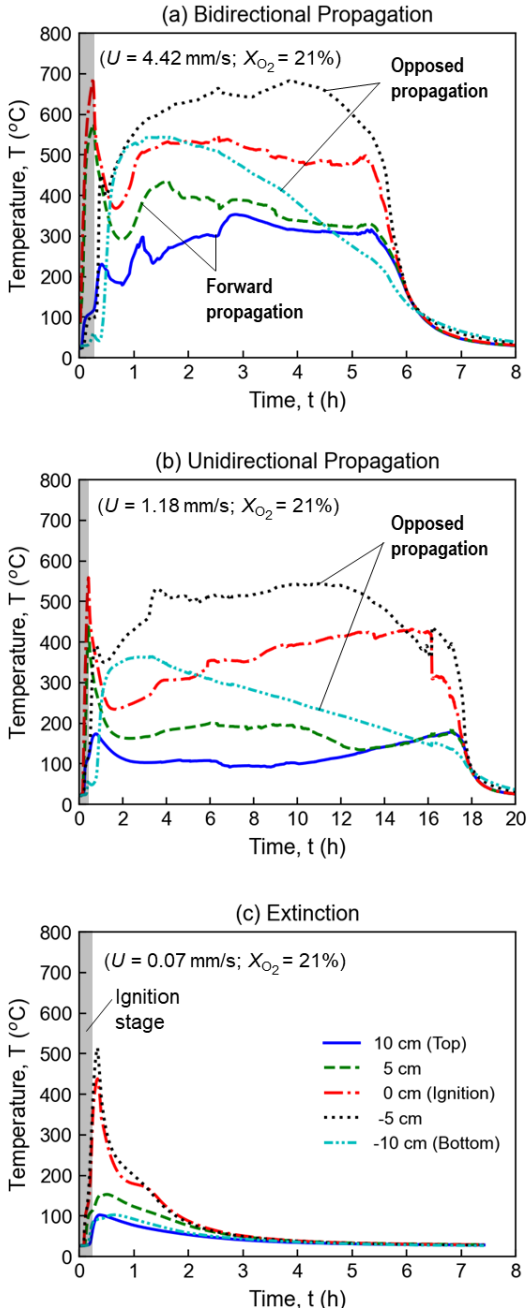

Fig. 2. Temperatures profiles at different airflow (X_{O_2}= 21%) velocities, (a) *U*=4.42 mm/s with a bidirectional propagation, (b) *U*=1.18 mm/s with a unidirectional propagation, and (c) *U*=0.07 mm/s without smoldering propagation, where the 15 min is the ignition heating stage.

Fig. 2(b) shows that as the airflow velocity is decreased to 1.2 mm/s, the bidirectional smoldering propagation disappears, where the measured temperature above the ignition zone is lower than the minimum smoldering temperature (~250 °C) [12]. Under such oxygen-limited conditions, the smoldering front only propagates towards the gas flow from the bottom (opposed), as ideally illustrated in Fig. 3(b). As the oxygen is almost consumed by the downward (or opposed) smoldering front, no excess oxygen is left to sustain another upward (or forward) smoldering propagation. After the test, an ash layer together with a thick layer of virgin fuel remained in the reactor, so that not all the peat and char were consumed, resulting in a lower burning mass loss (discussed more in Section 3.3).

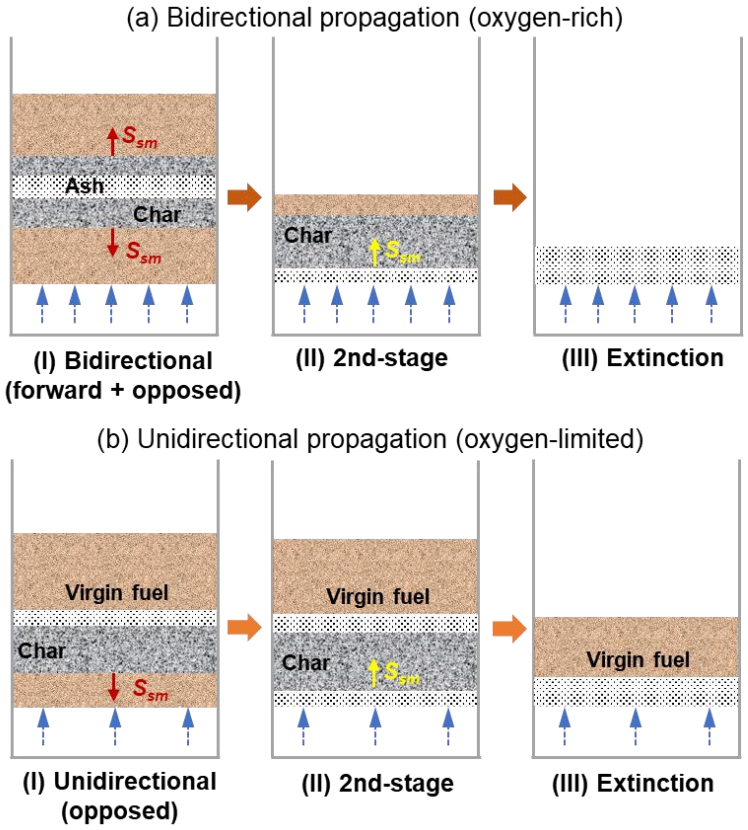

Fig. 3. Schematic diagrams of (a) bidirectional smoldering propagation and (b) unidirectional propagation under different oxygen conditions.

Further decreasing the airflow velocity, eventually, smoldering combustion cannot be sustained. Fig. 2(c) shows the temperature profile of a no-propagation case, where the forced airflow velocity is 0.07 mm/s. During the ignition process, the temperature near the coil heater also reached about 500 °C, but once the

heater was off, it kept decreasing to the ambient temperature without strong fluctuation. Further increasing the ignition duration to 30 and 45 min, smoldering propagation still did not occur, so the applied airflow velocity is below the smoldering limit of this fuel.

3.2. Oxygen supply limit for smoldering

Fig. 4(a) summarizes the experimental results of the minimum internal flow velocity (U_{min}) to sustain smoldering propagation under different oxygen concentrations (X_{O_2}). The hollow, semi-solid, and solid markers represent the cases of "no propagation," "unidirectional propagation," and "bidirectional propagation" of smoldering fire, respectively. As expected, the boundary of sustaining bidirectional propagation is much higher than that of sustaining unidirectional propagation. For example, with a forced airflow ($X_{O_2} = 21\%$), the minimum flow velocities to sustain bidirectional and unidirectional propagation are 2.9 mm/s and 0.3 mm/s, respectively.

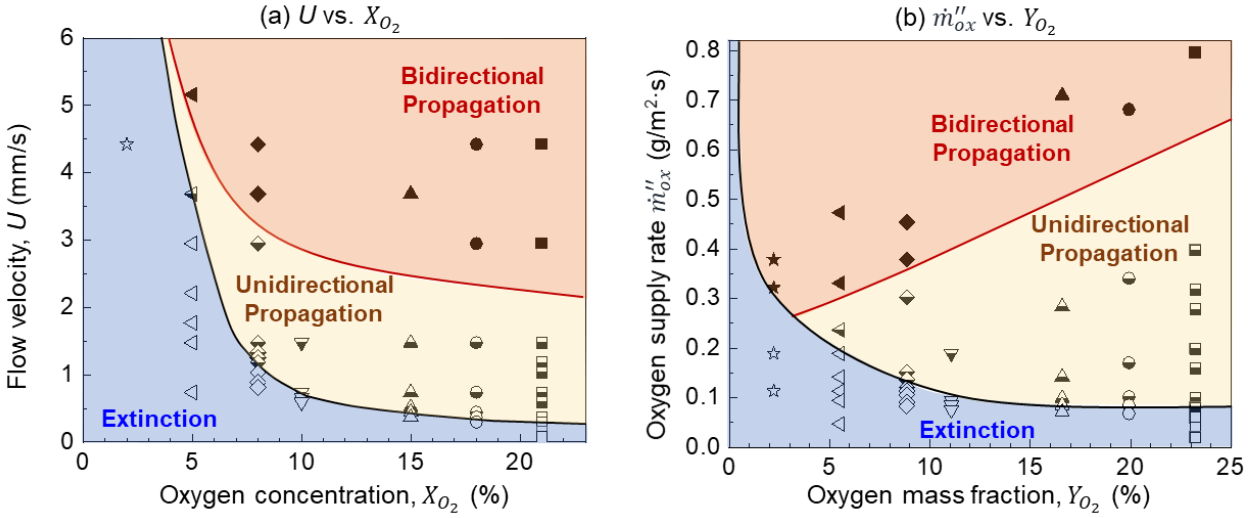

Fig. 4. (a) Minimum flow velocity (U_{min}) vs. oxygen concentration (X_{O_2}) and (b) minimum oxygen mass flow rate ($\dot{m}''_{ox,min}$) vs. oxygen mass fraction (Y_{O_2}).

Moreover, the required oxidizer flow velocities for both smoldering-propagation modes increase as the oxygen concentration decreases. For example, if the oxygen concentration is decreased from 21% to 10%, the minimum oxidizer flow velocity to sustain unidirectional propagation will increase by over two times from 0.3 mm/s to 0.7 mm/s.

Further reducing the oxygen concentration to 2%, smoldering combustion can still survive when the flow rate exceeds 12.5 mm/s. Fig. 5 shows temperature profiles of a successful smoldering propagation under 2% oxygen concentration. To the best of the authors' knowledge, this is the lowest oxygen concentration reported for smoldering fire. It is reasonable because strong exothermic char oxidation still occurs at 2% oxygen concentration, as shown in the thermogravimetric data (Fig. A1). In other words, the limiting oxygen concentration (LOC) for smoldering peat fire is below 2%. Therefore, the minimum oxygen concentration (MOC) for smoldering peat is about 1.5 ± 0.5%. Such a low LOC of smoldering fire helps explain why underground smoldering peat fire can be sustained in the deep soil layers for months [3].

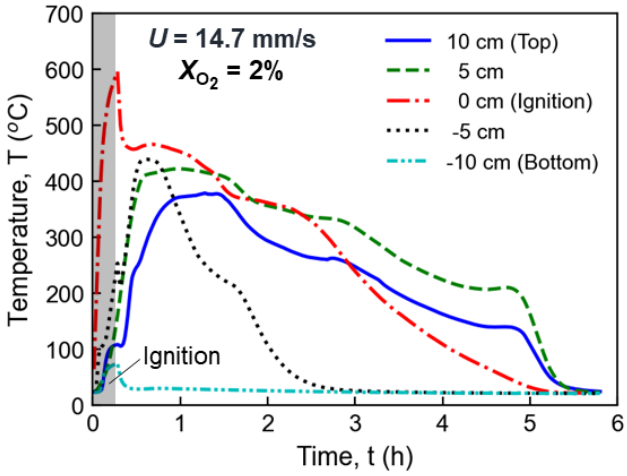

Fig. 5. Temperature profile at a flow velocity of U = 14.7 mm/s and oxygen concentration of X_{O_2}= 2%, where the 15 min is the ignition heating stage.

Herein, empirical correlations between the minimum flow velocity and oxygen concentration can be formulated as

$$U_{min} = \begin{cases} \dfrac{0.06}{X_{O_2} - MOC} & \text{(unidirectional)} \quad (2a) \\ \dfrac{0.06}{X_{O_2} - MOC} + 2 & \text{(bidirectional)} \quad (2b) \end{cases}$$

where the unit of the internal flow velocity is mm/s, and R^2 of the fitting is 0.97. This fitting is selected based on the theoretical analysis in Section 3.4. Note that for using these correlations, the oxygen concentration has to be larger than the MOC (≈ 1.5%); otherwise, it has no physical meaning.

At 2% oxygen concentration, the unidirectional propagation can no longer be observed. When the oxidizer flow is very fast, it does not have sufficient time to fully react with the downward (or opposed) smoldering front. Thus, there is always a large amount of unreacted oxygen leaking to the upward smoldering front to form a bidirectional smoldering propagation. In other words, the boundaries of these two propagation modes will merge in a large oxygen supply rate (see Fig. 4b).

Fig. 4(b) further summarizes the minimum oxygen supply rates ($\dot{m}''_{O_2,min}$) to sustain different smoldering propagation modes under different oxygen mass fractions (Y_{O_2}). For the oxygen mass fraction above 10%, the extinction limit of smoldering changes only slightly and approaches a minimum value of 0.08 ± 0.01 g/m^2·s, which could be defined as the minimum oxygen supply rate to sustain a smoldering propagation. Note that the minimum value of oxygen supply rate may still decrease slightly as the oxygen mass fraction increases above atmospheric value, which needs more verifications in future work. As the oxygen mass fraction further drops below 10%, the minimum oxygen supply rate for (unidirectional) smoldering propagation gradually increases to 0.25 ± 0.05 g/m^2·s at X_{O_2}=2%.

Based on Eqs. (1) and (2), we have an empirical correlation between the minimum oxygen supply rate and oxygen level as

$$\dot{m}''_{O_2,min} = \rho_g Y_{O_2} U_{min} \approx \begin{cases} \dfrac{0.08 Y_{O_2}}{Y_{O_2} - MOC} & \text{(unidirectional)} \quad \text{(3a)} \\ \dfrac{0.08 Y_{O_2}}{Y_{O_2} - MOC} + 2.5 Y_{O_2} & \text{(bidirectional)} \quad \text{(3b)} \end{cases}$$

where MOC = 1.5 ± 0.5% for the test peat fuel, and R^2 of the fitting is above 0.9 because the difference between oxygen volume and mass fractions are relatively small ($X_{O_2} \approx Y_{O_2}$).

For the boundary between bidirectional and unidirectional smoldering-propagation modes, the limiting oxidizer flow velocity (U) also gradually increases with the decreasing oxygen concentration, as shown in Fig. 4(a). Such a boundary is almost parallel to the lower boundary of the extinction limit with a constant gap of about 2 mm/s. It is possible that a minimum flow residence time is required to enable a bidirectional smoldering propagation. On the other hand, as the oxygen concentration decreases, both the limiting value of the oxygen supply rate and the gap of the unidirectional-propagation regime decrease (see Fig. 4(b)).

3.3. Mass loss and smoldering temperature

In addition to the oxygen limits of smoldering, the mass losses and peak smoldering temperatures are also summarized in Fig. 6, which may help understand the near-limit smoldering behavior and extinction limits of smoldering combustion. Fig. 6(a) summarizes all mass-loss fractions, where solid, semi-solid, and hollow symbols indicate bidirectional propagation, unidirectional propagation, and extinction cases, respectively. First of all, the mass loss during the forced ignition process is quantified, which is around 9.0% (24.3 g out of 270 g). Afterwards, the mass loss with different flow conditions can be divided into three regions with different propagation modes.

For the bidirectional propagation, a larger mass loss of over 70% was obtained. As discussed in Section 3.2 and illustrated in Fig. 3, the occurrence of bidirectional smoldering propagation is caused by excess oxygen supply. After the test, only a thin ash layer was observed at the bottom of the reactor, thus resulting in a larger mass loss close to the organic fraction of fuel (~97%). Comparatively, the unidirectional smoldering propagation can consume 35-70% of the fuel mass. Because the oxygen supply is relatively limited, a layer of virgin unburnt fuel remains after extinction, resulting in a lower mass loss. Also, the range of mass loss fraction for unidirectional propagation increases with the oxygen concentration, showing a similar trend to the oxygen supply rate in Fig. 4(b).

Finally, for cases of no smoldering propagation, a mass loss of 10-35% could still be achieved. The additional mass loss beyond ignition is caused by a weak char oxidation process that could still survive in the preheated ignition regions. Nevertheless, due to the lack of oxygen, such a smoldering front could not propagate out (i.e., local burning only). Note that the mass loss generally increases with the flow velocity because of a better oxygen supply. However, as the flow velocity further increases, the mass loss may also start to decrease because of the dominant convective heat loss (see more discussion in Section 3.4).

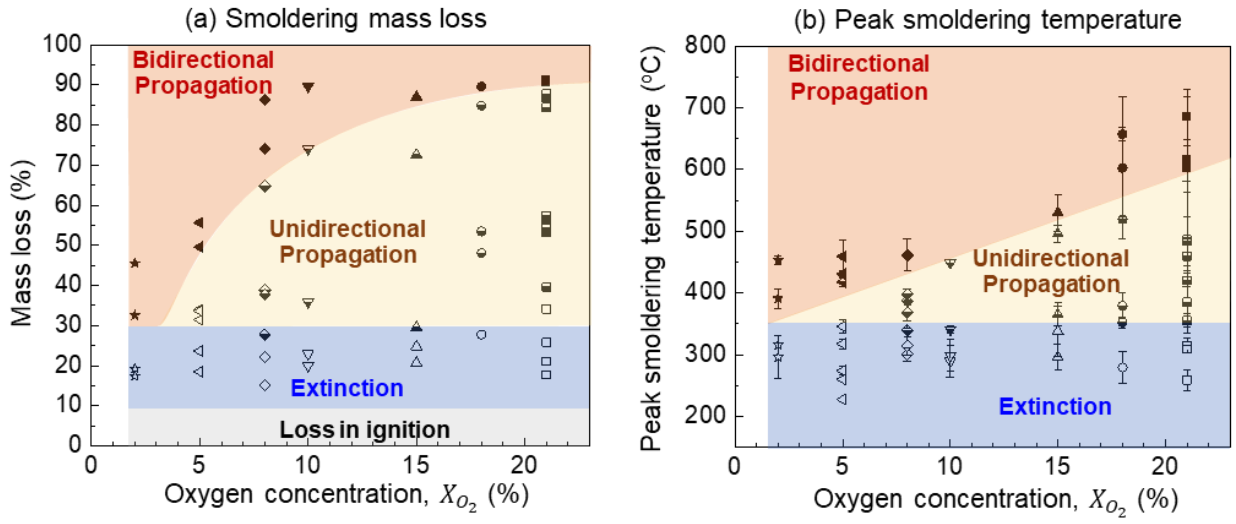

Fig. 6. (a) Mass loss and (b) the peak temperature during different smoldering-propagation modes.

Fig. 6(b) shows the effect of flow velocity and oxygen concentration on the measured peak smoldering temperature. For this organic peat soil, the maximum smoldering temperature is about 700 °C, which is close to the literature values [12,15,33]. Moreover, the smoldering temperature increases as the oxygen concentration or internal flow velocity increases. For example, given an oxygen concentration of 18%, as the flow velocity increases from 0.4 mm/s to 4.4 mm/s, the smoldering temperature increases from 352 °C to 658 °C. It is because a stronger oxygen supply can lead to a stronger char oxidation process.

On the other hand, as oxygen concentration and flow velocity decrease, the smoldering temperature gradually decreases. Eventually, at the extinction limit, there is a global minimum smoldering temperature of about 300 °C, regardless of the oxygen concentration and flow velocity. Such a minimum is close to the threshold temperature for char oxidation found in the thermogravimetric analysis and similar to the literature data [12,34]. Note that under an extremely oxygen-limited condition, the smoldering front may only burn locally or break up into separated combustion fronts without consuming all the fuel in the same cross section (namely, the fingering-spread phenomenon [35]). Then, the physical meaning and accuracy of smoldering propagation rate measured by a limited number of thermocouples are questionable, so they are not discussed in this work. In our future work, a longer reactor will be designed with more thermocouples to further quantify the local and global propagation rates under low oxygen supply.

3.4. Analysis of minimum oxygen supply

To scientifically explain the relationship between the minimum flow velocity (U_{min}), minimum oxygen mass flow rate ($\dot{m}''_{O_2,min}$) and oxygen fraction (X_{O_2} or Y_{O_2}), a simplified energy conservation equation is applied to a (unidirectional and opposed) propagating smoldering front, as shown in Fig. 7. The unidirectional opposed smoldering propagation requires the smallest oxygen supply, so it defines the minimum oxygen-supply condition.

At the extinction limit, the heat generated from the net heterogenous smoldering reactions ($\dot{q}''_{sm}$) should just balance the heat loss from water evaporation ($\dot{q}''_{MC}$), internal flow convection ($\dot{q}''_{conv}$), and environmental heat losses ($\dot{q}''_{e}$) such as cold walls and ambient as

$$\dot{q}''_{sm,min} = \dot{q}''_{MC} + \dot{q}''_{conv} + \dot{q}''_{e} \tag{4}$$

where the minimum oxidation heat generated is

$$\dot{q}''_{sm,min} = \dot{m}''_{O_2,min}\Delta H_{ox} = \rho_g (UY_{O_2})_{min}\Delta H_{ox} \tag{5}$$

where ρ_g is the density of oxidizer flow, and ΔH_{ox} is the heat of smoldering oxidation. Therefore, the minimum oxidizer flow velocity can be derived as

$$U_{min} = \frac{\dot{q}''_{MC} + \dot{q}''_{conv} + \dot{q}''_{e}}{\rho_g Y_{O_2}\,\Delta H_{ox}} \propto \frac{1}{Y_{O_2}} \tag{6}$$

which shows that the minimum gas flow velocity is inversely proportional to the oxygen concentration ($X_{O_2} \approx Y_{O_2}$) in Eq. (2a). Thus, the overall trend of experimental data in Fig. 4(a) is successfully explained, and more detailed influence of convective cooling under low oxygen concentration will be further discussed.

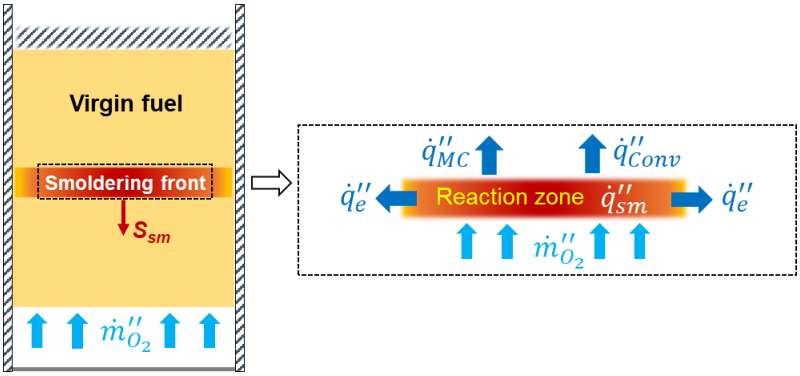

Fig. 7. Schematics for energy conservation in propagating smoldering front.

Further reorganizing the energy equation, the minimum oxygen supply rate can be expressed as

$$\dot{m}''_{O_2,min} = U_{min}\rho_g Y_{O_2} = \frac{\dot{q}''_{MC} + \dot{q}''_{conv} + \dot{q}''_e}{\Delta H_{ox}} \quad (7a)$$

As the oxygen concentration decreases below 10%, the required internal flow velocity increases significantly (see Fig. 4a), and its convective cooling ($\dot{q}''_{conv}$) becomes important [36], as

$$\dot{q}''_{conv} = h(T_{sm} - T_\infty) = Nu\left(\frac{k}{D}\right)(T_{sm} - T_\infty) \quad (8)$$

$$Nu \propto Re^m Pr^n \propto (UD/\nu)^m(\nu/\alpha)^n \propto U^m \quad (9)$$

where h is convective heat transfer coefficient, T_∞ is ambient temperature, D is the pore size, ν is momentum diffusion, α is thermal diffusivity, and $0 < m < 1$ [37]. In other words, the convective cooling of the internal flow also increases with the flow velocity, which becomes significant for limiting cases with low oxygen concentration and large internal flow rate. Thus, with low oxygen concentration and large oxidizer flow rate, the minimum oxygen supply rate can be described as

$$\dot{m}''_{O_2,min} = U_{min}\rho_g Y_{O_2} \propto \dot{q}''_{conv} \propto U_{min}^m \propto \left(Y_{O_2}\right)^{\frac{m}{m-1}} \quad (Y_{O_2} < 10\%) \quad (7b)$$

Specifically, with $m = 0.5$, we have $U_{min} \propto 1/Y_{O_2}^2$ and $\dot{m}''_{O_2,min} \propto 1/Y_{O_2}$. Therefore, the minimum oxygen supply rate increases with the flow velocity and decreases with the oxygen concentration. This successfully explains the experimental trend in Fig. 4(b), when the oxygen mass fraction (Y_{O_2}) is smaller than 10%.

On the other hand, as the oxygen mass flux further increases, the required flow velocity will gradually decrease (see Fig. 4a). Eventually, the minimum required flow velocity will be tiny, so the convective heat loss becomes negligible as

$$\dot{m}''_{O_2,min} = \frac{\dot{q}''_{MC} + \dot{q}''_{conv} + \dot{q}''_e}{\Delta H_{ox}} \approx \frac{\dot{q}''_{MC} + \dot{q}''_e}{\Delta H_{ox}} = \text{const.} \quad (Y_{O_2} \geq 10\%) \quad (7c)$$

As a result, the minimum oxygen supply rate approaches a constant if the fuel condition (e.g., moisture) and reactor configurations are fixed. This well explains the $\dot{m}''_{O_2,min}$ =0.08 g/m^2·s found in the experiment when the oxygen mass fraction is larger than 10% (see Fig. 4(b)).

Eq. (7c) also indicate that the value of this minimum oxygen supply rate changes with the fuel. For example, the heat of oxidation (ΔH_{ox}) depends on the fuel type and chemistry, the thermal conductivity of the fuel bed changes the environmental heat losses ($\dot{q}_e''$), and a higher oxygen supply rate is expected due to the increases in $\dot{q}_{MC}''$. Therefore, additional measurements are needed for different fuel types and fuel-bed conditions to form a database that can help evaluate and rank their smoldering fire hazards.

4. Conclusions

In this work, we experimentally quantify the limiting oxygen supply to sustain different smoldering propagation modes. After ignition in the middle of the fuel bed, by increasing the flow velocity, smoldering transitions from the unidirectional (opposed) propagation to the bidirectional (opposed + forward) propagation. The minimum oxidizer flow velocities to sustain both modes of propagation decrease as the oxygen concentration increases. The minimum oxygen supply rate for stable smoldering propagation decreases with the oxygen concentration and approaches a critical value of 0.08 g/m^2·s at ambient oxygen level. Moreover, smoldering is found to survive at an extremely low oxygen concentration of 2%, so the value of minimum oxygen concentration (if exists) is even smaller.

As the oxygen concentration and oxidizer flow velocity increase, both the mass loss and peak smoldering temperature increase. Meanwhile, the minimum smoldering temperature is found to be around 300 ^{o}C, independent of the oxygen supply conditions. A simplified heat transfer analysis successfully explains the relationship between the minimum oxygen supply rate and oxygen concentration of smoldering propagation. Future numerical simulations are needed to reveal the underlying physical and chemical process of smoldering propagation under different flow conditions. This work provides vital information about the persistence of smoldering propagation and underground peat fire.

Declaration of Competing Interest

The authors declare that there is no conflict of interest.

Acknowledgments

This research is funded by the National Natural Science Foundation of China (NSFC) No. 51876183.

CRediT Authorship Contribution Statement

Yunzhu Qin: Investigation, Data Curation, Writing-original draft, Formal analysis, Resources. **Yuying Chen**: Formal analysis, Resources. **Shaorun Lin**: Investigation, Writing-review & editing, Formal analysis, Resources. **Xinyan Huang:** Conceptualization, Supervision, Methodology, Writing-review & editing, Formal analysis, Funding acquisition.

References

[1] Rein G. Smoldering Combustion. *SFPE Handbook of Fire Protection Engineering* 2014;2014:581–603.

[2] Ohlemiller TJTJ. Modeling of smoldering combustion propagation. *Progress in Energy and Combustion Science* 1985;11:277–310.

[3] Rein G. Smouldering Fires and Natural Fuels. In: Claire M. Belcher, editor. Fire Phenomena in the Earth System, New York: John Wiley & Sons, Ltd.; 2013, p. 15–34.

[4] Santoso MA, Christensen EG, Yang J, Rein G. Review of the Transition From Smouldering to Flaming Combustion in Wildfires. *Frontiers in Mechanical Engineering* 2019;5.

[5] Huang X, Rein G. Interactions of Earth's atmospheric oxygen and fuel moisture in smouldering wildfires. *Science of the Total Environment* 2016;572:1440–6.

[6] Quintiere J. Principles of Fire Behaviour. New York: Alar Elken; 1997.

[7] Rein G, Huang X. Smouldering wildfires in peatlands, forests and the arctic: Challenges and perspectives. *Current Opinion in Environmental Science and Health* 2021;24:100296.

[8] Chen Y, Liang Z, Lin S, Huang X. Limits of sustaining a flame above smoldering woody biomass. *Combustion Science and Technology* 2022.

[9] Yermán L, Wall H, Torero JL. Experimental investigation on the destruction rates of organic waste with high moisture content by means of self-sustained smoldering combustion. *Proceedings of the Combustion Institute* 2017;36:4419–26.

[10] Torero JL, Gerhard JI, Martins MF, Zanoni MAB, Rashwan TL, Brown JK. Processes defining smouldering combustion: Integrated review and synthesis. *Progress in Energy and Combustion Science* 2020;81:100869.

[11] Lin S, Yuan H, Huang X. A computational study on the quenching and near-limit propagation of smoldering combustion. *Combustion and Flame* 2022;238:111937.

[12] Lin S, Huang X. Quenching of smoldering: Effect of wall cooling on extinction. *Proceedings of the Combustion Institute* 2021;38:5015–22.

[13] Huang X, Rein G. Computational study of critical moisture and depth of burn in peat fires. *International Journal of Wildland Fire* 2015;24:798–808.

[14] Hadden R, Rein G. Chapter 18 - Burning and Water Suppression of Smoldering Coal Fires in Small-Scale Laboratory Experiments. In: Stracher GB, Prakash A, Sokol EVBT-C and PFAGP, editors., Amsterdam: Elsevier; 2011, p. 317–26.

[15] Lin S, Cheung YK, Xiao Y, Huang X. Can rain suppress smoldering peat fire? *Science of the Total Environment* 2020;727:138468.

[16] Ramadhan ML, Palamba P, Imran FA, Kosasih EA, Nugroho YS. Experimental study of the effect of water spray on the spread of smoldering in Indonesian peat fires. *Fire Safety Journal* 2017;91:671–9.

[17] Lin S, Chow TH, Huang X. Smoldering propagation and blow-off on consolidated fuel under external airflow. *Combustion and Flame* 2021;234:111685.

[18] Moussa N a., Toong TY, Garris C a. Mechanism of smoldering of cellulosic materials. *Symposium (International) on Combustion* 1977;16:1447–57.

[19] Schmidt M, Lohrer C, Krause U. Self-ignition of dust at reduced volume fractions of ambient oxygen. *Journal of Loss Prevention in the Process Industries* 2003;16:141–7.

[20] Malow M, Krause U. Smouldering combustion of solid bulk materials at different volume fractions of oxygen in the surrounding gas. *Fire Safety Science* 2008;9:303–14.

[21] Belcher CM, Yearsley JM, Hadden RM, Mcelwain JC, Rein G. Baseline intrinsic flammability of Earth ' s ecosystems estimated from paleoatmospheric oxygen over the past 350 million years. *Proceedings of the National Academy of Sciences* 2010;107:22448–22453.

[22] Hadden RM, Rein G, Belcher CM. Study of the competing chemical reactions in the initiation and spread of smouldering combustion in peat. *Proceedings of the Combustion Institute* 2013;34:2547–53.

[23] Richter F, Jervis FX, Huang X, Rein G. Effect of oxygen on the burning rate of wood. *Combustion and Flame* 2021;234:111591.

[24] Wang H, van Eyk PJ, Medwell PR, Birzer CH, Tian ZF, Possell M. Effects of Oxygen Concentration on Radiation-Aided and Self-sustained Smoldering Combustion of Radiata Pine. *Energy & Fuels* 2017;31:8619–30.

[25] Bar-Ilan A, Rein G, Walther DC, Fernandez-Pello AC, Torero JL, Urban DL. The effect of buoyancy on opposed smoldering. *Combustion Science and Technology* 2004;176:2027–55.

[26] Walther DC, Carlos Fernandez-Pello A, Urban DL. Small-scale smoldering combustion experiments in microgravity. *Proceedings of the Combustion Institute* 1996;26:1361–8.

[27] Yamazaki T, Matsuoka T, Nakamura Y. Near-extinction behavior of smoldering combustion under highly vacuumed environment. *Proceedings of the Combustion Institute* 2019;37:4083–90.

[28] Yamazaki T, Matsuoka T, Li Y, Nakamura Y. Applicability of a Low-Pressure Environment to Investigate Smoldering Behavior Under Microgravity. *Fire Technology* 2020.

[29] Lin S, Sun P, Huang X. Can peat soil support a flaming wildfire? *International Journal of Wildland Fire* 2019;28:601–13.

[30] Hu Y, Christensen EG, Amin HMF, Smith TEL, Rein G. Experimental study of moisture content effects

on the transient gas and particle emissions from peat fires. *Combustion and Flame* 2019;209:408–17.

[31] Yan H, Fujita O. Experimental investigation on the smoldering limit of scraps of paper initiated by a cylindrical rod heater. *Proceedings of the Combustion Institute* 2019;37:4099–106.

[32] Xie Q, Zhang Z, Lin S, Qu Y, Huang X. Smoldering Fire of High-Density Cotton Bale Under Concurrent Wind. *Fire Technology* 2020;56:2241–56.

[33] Huang X, Restuccia F, Gramola M, Rein G. Experimental study of the formation and collapse of an overhang in the lateral spread of smouldering peat fires. *Combustion and Flame* 2016;168:393–402.

[34] Huang X, Rein G. Upward-and-downward spread of smoldering peat fire. *Proceedings of the Combustion Institute* 2019;37:4025–33.

[35] Huang X, Gao J. A review of near-limit opposed fire spread. *Fire Safety Journal* 2021;120:103141.

[36] Incropera FP. Principles of heat and mass transfer. John Wiley; 2007.

[37] Wang S, Lin S, Liu Y, Huang X, Gollner MJ. Smoldering ignition using a concentrated solar irradiation spot. *Fire Safety Journal* 2022;129.

Appendix

The thermogravimetric tests were conducted using PerkinElmer STA6000 under five oxygen concentrations by mixing air and N_2: 21% (air), 10%, 5%, 2% and 0% (N_2). In this study, it exposes 2-3 mg samples to a temperature ramp of 30 °C/min from room temperature to 800 °C. For each scenario, tests were repeated at least twice to ensure good experimental repeatability. Fig. A1 (a) shows the derivative thermogravimetric (DTG) curves of organic peat soils against the temperatures in different test scenarios. For all tests, the first mass loss stage below 200 °C is mainly due to the dehydration process, which accounts for less than 10% of the total mass loss. Basically, except for the drying stage at the temperature below 100 °C, there are two curve peaks with fast mass loss. One peak represents the pyrolysis process, at around 270 °C where the mass loss rate rises rapidly. In this process, peat samples absorb heat and decompose into pyrolysis gases and char. It shows that the pyrolysis temperatures of the samples under different oxygen conditions are very close.

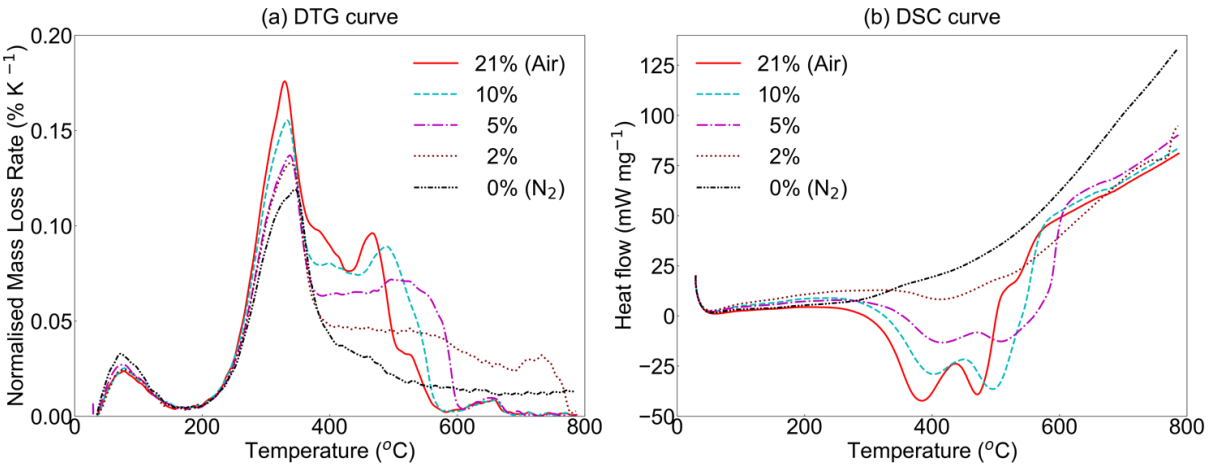

Fig. A1. (a) DTG and (b) DSC curves of tested peat soil in different oxygen concentrations.

However, the peak mass loss rate increases as the oxygen concentration increases. It indicates that some oxidation process should also exist in this temperature (~ 320 ^{o}C) whose reaction rate increases with the oxygen concentration. With the temperature rising, the fuel is gradually decomposed, and then, oxidation turns into the main reaction causing the mass loss. It is worth noting that oxidation reaction was observed at any oxygen concentration (excluding N_2 without any oxygen) in this study. That is, smoldering can occur under extremely low oxygen concentration (below 2%, as shown in Fig. 5). From Fig. A1(a), we can also see that reducing the oxygen concentration does not affect the final total mass loss unless all oxygen is removed (i.e., pure N_2 environment). Nevertheless, a lower oxygen concentration will significantly slow down the rates of oxidation and smoldering propagation.

Fig. A1(b) shows the amount of heat required to increase the temperature of the sample, which provides a reference for the temperature reaction that occurs and the heat released. Basically, decreasing the oxygen concentration increases the temperature required for the reaction and decreases the peak exothermic rate of the reaction. The total smoldering heat of the whole temperature range (up to 800 ^{o}C) is calculated to be almost constant (about 12.6 MJ/kg). Nevertheless, if the maximum smoldering temperature is lower, the released heat of smoldering will be smaller.